grains present in the quartzite. It has been reported that sulfate-bearing solutions could effectively mobilize the REE without fractionating them[13]. In the uppermost friable zones, a small flattening of HREE pattern has been observed. This could be due to the possible presence of carbonate complexes released by weathering of organic materials in the presence of meteoric water and due to the greater solubility of HREE in carbonate complexes[14].

From the geochemical characteristics of the weathering rinds of the Delhi quartzites we infer that, (i) rare earth elements can be mobilized in upper zones and retained in the lower moderately weathered zones during clay forming processes; (ii) presence of acid and sulfate ions in the weathering solutions can mobilize the REE without any fractionation; (iii) similar weathering processes accompanied by sedimentary redistribution processes could result in the formation of silica-rich quartzite with low REE abundance from their protoliths; and (iv) longer time span for the weathering and redistribution within the profile could have been an important process for the *in situ* maturation and production of silica-rich sediments, (e.g. mature quartzites) under stable cratonic situations.

1. Chalcraft, D. and Pye, K., *Z. Geomorphol. N. F.*, 1984, **28**, 321–332.
2. Wray, R. A. L., *Earth Sci. Rev.*, 1997, **42**, 137–160.
3. Goldich, S. S., *J. Geol.*, 1938, **46**, 17–58.
4. Nesbitt, H. W., Fedo, C. M. and Young, G. M., *J. Geol.*, 1997, **105**, 177–191.
5. Nesbitt, H. W. and Markovics, G., *Geochim. Cosmochim. Acta*, 1997, **61**, 1653–1670.
6. Suttner, L. J., Basu, A. and Mack, G. H., *J. Sediment. Petrol.*, 1981, **51**, 1235–1246.
7. Franzinelli, E. and Potter, P. E., *J. Geol.*, 1983, **91**, 23–29.
8. Tripathi, J. K. and Rajamani, V., *Chem. Geol.*, 1989, **155**, 265–278.
9. Tripathi, J. K., Unpublished Ph D thesis, Jawaharlal Nehru University, New Delhi, 1997, p. 153.
10. Nesbitt, H. W. and Young, G. M., *Geochim. Cosmochim. Acta*, 1984, **97**, 129–147.
11. McLennan, S. M., *J. Geol.*, 1993, **101**, 295–303.
12. Morris, R. C. and Fletcher, A. B., *Nature*, 1987, **330**, 558–561.
13. Wood, S. A., *Chem. Geol.*, 1990, **82**, 159–186.
14. Nesbitt, H. W., *Nature*, 1979, **279**, 206–210.

ACKNOWLEDGEMENTS. J.K.T. thanks Manoj Kumar Mohanta and T. S. Giritharan for their cooperation during geochemical data generation. He also thanks JNU/UGC and CSIR for scholarships during his Ph D and Research Associateship respectively.

Received 1 July 1998; revised accepted 1 February 1999

Petrogenesis of the protolith for the Tirodi gneiss by A-type granite magmatism: The geochemical evidence

M. V. Subba Rao, B. L. Narayana, V. Divakara Rao and G. L. N. Reddy

National Geophysical Research Institute, Hyderabad 500 007, India

In the Central Indian region, the Tirodi gneisses occur intimately associated with the Sausar Group metasediments. The protoliths for these gneisses might have originated by rift-related intracontinental felsic A-type (anorogenic) magmatism. The geochemical signatures in them like high Zr + Nb + Y + Ce, Ga/Al, Zr/Ni, Rb/Sr and Y/Sc, are quite similar to the A-type granite characteristics and point to the derivation of the protoliths by the melting of lower crustal dehydrated assemblages at high temperatures attained as a result of possible ponding of basaltic magma/magma underplating. The occurrence of mafic rocks related to subduction zone magmatism and back-arc environment in the vicinity of these gneisses in the Central Indian region attest to such an origin for the protoliths of the Tirodi gneisses.

IN the Central Indian region, the Tirodi gneiss is a major lithological unit (Figure 1). These quartzo–feldspathic granitic gneisses are intimately associated with the metasediments of the Sausar Group. The basement–cover relationships of the granitic gneisses and the associated metasediments are obscured by the extensive migmatization at several places especially at the peripheries. There exist two schools of thought regarding the mutual relationships of the Tirodi gneisses and the metasediments of the Sausar Group. One school subscribes to the theory that the Tirodi gneisses constitute the basement on which the sediments of the Sausar Group have been deposited, while the other group of workers are of the opinion that the protoliths of the Tirodi gneisses intruded into the sediments of the Sausar Group[1–3]. Rb–Sr isotopic studies[4] could not help much in resolving this issue. In the absence of reliable and quality trace and rare earth element (REE) data, the limited studies so far on the Tirodi gneisses, could not focus on the petrogenetic aspects of the protoliths of these gneisses.

In this study, an attempt is made to throw some light on the nature of the magmatism that led to the formation of the protoliths of the Tirodi gneisses, based on a comprehensive new set of major and trace element (including REE) data of 20 representative samples of the Tirodi gneisses. Further the possible petrogenesis of the protoliths is evaluated.

Tirodi gneiss is a part of the Central Indian gneissic complex (Figure 1) and is exposed to the north of the supposed Central Indian suture (CIS). The samples studied are mainly from areas surrounding the mining

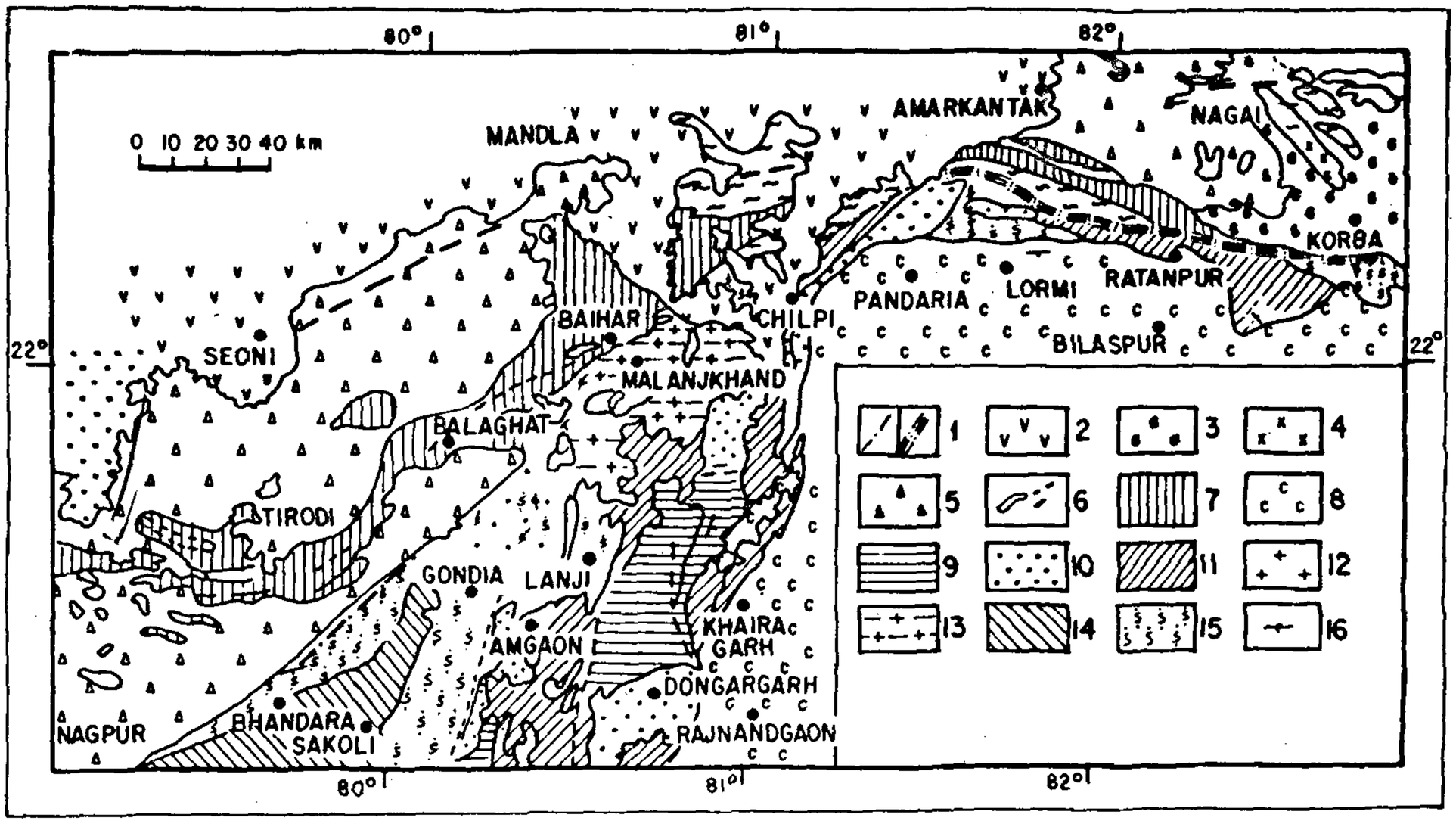

Figure 1. Geological map of the Central Indian region, showing the location of the Tirodi gneiss. 1, CIS/Mylonite zone; 2, Deccan basalt and Lameta formation; 3, Gondwana group; 4, Granites; 5, Tirodi gneiss; 6, Granulites; 7, Sausar metasediments; 8, Chattisgarh group; 9, Khairagarh group; 10, Chilpi group; 11, Nandagaon group; 12, Dongargarh granitoid; 13. Malanjkhand granitoid; 14, Sakoli group; 15, Amgaon gneisses; 16, Attitude of bedding.

Table 1. Representative major and trace element compositions of the Tirodi gneiss*

Wt%	MC52	MC53	MC67	MC76	MC77	MC80	MC97	MC125
SiO_2	59.07	69.05	72.47	75.49	62.95	68.20	63.66	75.69
Al_2O_3	16.18	15.28	14.25	13.55	15.05	14.99	16.56	13.83
TiO_2	1.62	1.08	0.64	0.17	1.02	0.85	0.70	0.03
CaO	2.63	1.63	1.91	0.65	0.69	2.26	1.24	0.88
MgO	2.47	0.83	0.67	0.03	5.23	1.83	0.72	0.03
$Fe_2O_3^T$	9.43	3.23	2.95	1.04	8.03	4.94	6.31	0.98
Na_2O	3.07	2.46	3.06	2.79	1.79	2.78	3.31	3.57
K_2O	5.04	6.85	4.96	6.58	6.00	4.62	8.14	5.21
MnO	0.06	0.04	0.03	0.02	0.05	0.06	0.14	0.05
P_2O_5	0.28	0.19	0.12	0.01	0.07	0.30	0.07	0.01
Total	99.85	100.64	101.06	100.33	100.88	100.83	100.84	100.28
A/CNK	1.06	1.03	1.08	1.06	1.40	1.09	1.00	1.05
(ppm)								
Sc	18	4	13	6	15	10	12	9
V	8	7	3	1	52	9	23	14
Cr	8	5	4	5	51	12	14	11
Ni	3	3	4	5	26	9	7	16
Cu	3	3	1	1	20	2	2	1
Ga	71	18	33	24	26	31	67	14
Rb	127	129	226	295	277	218	177	182
Sr	153	250	59	34	34	202	22	72
Y	104	9	84	55	10	26	78	49
Zr	877	17	756	330	127	308	385	130
Nb	35	17	13	9	16	15	281	1
Cs	1	1	2	3	8	5	1	1
Ba	893	1713	260	112	429	503	83	265
Hf	20	1	17	10	4	7	3	7
Ta	2	1	1	1	3	2	11	1
Th	100	1	48	63	23	27	3	8
U	5	1	7	7	3	1	1	1

*Complete set of data can be obtained from the authors.

Table 2. Representative rare earth element compositions of the Tirodi gneiss

(ppm)	MC52	MC53	MC67	MC76	MC77	MC80	MC97	MC125
La	264.54	39.81	92.00	45.16	40.82	58.12	96.75	5.21
Ce	388.18	58.21	149.04	98.81	72.92	119.90	155.05	22.55
Pr	45.39	7.66	18.02	11.06	8.89	17.47	23.57	3.26
Nd	122.03	20.79	50.15	30.32	30.58	32.79	83.15	9.34
Sm	21.83	3.94	9.18	6.44	6.84	5.67	15.38	3.05
Eu	1.79	2.16	0.54	0.37	0.97	0.76	0.49	0.59
Gd	16.80	3.51	7.17	4.70	4.26	5.03	10.55	2.66
Tb	2.99	0.37	1.31	0.86	0.83	0.94	1.98	0.68
Dy	18.91	1.69	8.63	5.59	2.75	6.47	12.18	5.13
Ho	2.50	0.31	1.87	1.29	0.37	0.57	1.86	1.07
Er	6.62	0.91	4.22	3.64	1.23	1.65	5.68	3.05
Tm	0.67	0.15	0.66	0.46	0.17	0.25	0.62	0.46
Yb	4.25	0.61	4.51	4.08	0.51	1.87	4.25	3.23
Lu	0.57	0.05	0.56	0.61	0.10	0.12	0.65	0.45
ΣREE	897.07	140.17	347.86	213.39	171.24	251.61	412.16	60.73
Ratio								
La_N/Yb_N	46.50	46.90	14.60	8.00	57.30	22.30	10.10	2.00
Ce_N/Yb_N	25.36	26.53	9.19	6.70	39.67	17.82	10.12	1.94
La_N/Sm_N	8.12	6.52	6.47	4.55	3.82	6.62	4.04	1.96
Gd_N/Yb_N	3.27	4.77	1.32	0.95	6.91	2.22	2.05	0.68
Eu/Eu*	0.28	1.78	1.20	0.21	0.54	0.44	0.12	0.63

town of Tirodi. These granitic gneisses are divided into grey and pink granitic gneisses which grade imperceptibly into each other. Pink gneisses cut across the grey gneisses and both are traversed by aplites and pegmatites. These gneisses show E–W trending foliation defined by parallelism of the micas and elongate feldspar and quartz grains. Migmatites of pink and grey colour are banded in appearance and are always associated with granitic gneisses but are less frequent. Ptygmatic folds of quartzo–feldspathic veins are common.

The essential mineral assemblages in these gneisses are quartz, microcline–microperthite and plagioclase. Deformation is not significant and no deformation textures are noticed. Antiperthite, chess-board albite and albite rims around plagioclase at the contact of k-feldspar are present. The plagioclase in these rocks varies from albite to andesine. The twin laws observed in plagioclase suggest magmatic origin for the protoliths of these gneisses while those of migmatites favour a metamorphic origin in the upper amphibolite facies. K-feldspars show ex-solution perthites indicating the high temperature condition of formation. Presence of antiperthites also suggests high grade metamorphic or anatectic conditions. Both biotite and muscovite form the micas. The accessories include zircon, apatite, sphene, tourmaline and magnetite.

Twenty representative samples of the Tirodi gneiss were analysed for major, trace and rare earth element compositions. Selected analyses are given in Tables 1 and 2. These gneisses are characterized by a wide range of compositions with SiO_2 ranging from 59.07% to 75.69 wt% (Av. 70.59%); with moderate to high Al_2O_3 (13.37 to 16.56%; Av. 14.86%); low to moderate concentrations of TiO_2 (0.03 to 1.62%; Av. 0.53%); low CaO (0.53 to 2.88%; Av. 1.44%); low MgO (except one sample which has high MgO concentration of 5.23%; 0.03 to 5.23%; Av. 0.82%); variable but moderate to high levels of alkalies (Na_2O range from 1.79 to 4.80%, Av. 3.12%; K_2O varies from 1.51 to 8.14%; Av. 5.61%) with low to moderate levels of $Fe_2O_3^T$ (0.85 to 9.43%; Av. 3.57%). The average composition of these gneisses are remarkably similar to the average A-type granite (Table 3). Thus, these compositions reflect on the petrogenetic aspects of these gneisses. Similarly the trace element compositions exhibit significant variations, particularly in the case of Rb, Sr, Y, Zr and to certain extent in Nb, Cs, Ba, Hf and Ta as also U and Th (Table 1). The Na_2O–K_2O relationship in these gneisses assigns a predominantly granite- to quartz-monzonite character to them (Figure 2). On the AFM ($Na_2O + K_2O$–$Fe_2O_3^T$–MgO) plot they depict a calc-alkaline character (Figure 3).

La_N/Sm_N which indicates LREE fractionation has a positive correlation with SiO_2. However, at higher SiO_2 levels the trend is not evident, with large variation in La_N/Sm_N. On the other hand Ce_N/Yb_N tends to be low at higher SiO_2 levels (Figure 4). Similarly Gd_N/Yb_N which is indicative of HREE fractionation has a broad negative correlation.

The chondrite-normalized rare earth element patterns of these gneisses suggest overall fractionation of REE (Figure 5); LREE enrichment and fractionation are evident ($Ce_N/Yb_N = 0.79$ to 49.98; Av. 14.77); significant negative Eu anomalies are discernible except in

Table 3. Range and average chemical compositions of the Tirodi gneiss and average compositions of different granite types

	Tirodi gneiss					
Wt%	Min	Max	Avg	A-type granite	I-type granite	S-type granite
SiO_2	59.07	75.69	70.59	73.60	67.98	69.08
Al_2O_3	13.37	16.56	14.86	12.69	14.49	14.30
TiO_2	0.03	1.62	0.53	0.33	0.45	0.55
CaO	0.53	2.88	1.44	1.09	3.78	2.49
MgO	0.03	5.23	0.82	0.33	1.75	1.82
Fe_2O_3	0.85*	9.43*	3.57*	0.99	1.27	0.73
FeO	–	–	–	1.72	1.27	3.23
Na_2O	1.79	4.80	3.12	3.34	2.95	2.20
K_2O	1.51	8.14	5.61	4.51	3.05	3.69
MnO	0.02	0.21	0.06	0.06	0.08	0.06
P_2O_5	0.01	0.30	0.09	0.09	0.11	0.13
A/CNK	1.00	1.47	1.08	1.03	0.96	1.18
Sc (ppm)	1.00	18.00	10.00	14.00	15.00	14.00
V	1.00	52.00	13.60	10.00	74.00	72.00
Cr	4.00	51.00	10.65	3.00	27.00	46.00
Ni	1.00	26.00	8.40	2.00	9.00	17.00
Cu	1.00	20.00	3.10	6.00	11.00	12.00
Ga	11.00	89.00	31.95	21.00	16.00	17.00
Rb	94.00	317.00	220.01	199.00	132.00	180.00
Sr	6.00	349.00	94.55	105.00	253.00	139.00
Y	9.00	111.00	50.90	76.00	27.00	32.00
Zr	17.00	877.00	346.60	342.00	143.00	170.00
Nb	1.00	281.00	31.30	22.00	9.00	11.00
Ba	83.00	1723.00	399.70	605.00	520.00	480.00
Th	1.00	100.00	35.60	105.00	16.00	19.00
U	1.00	14.00	4.15	23.00	3.00	3.00
La	5.21	264.54	76.63	55.00	29.00	31.00
Ce	12.83	388.18	130.93	134.00	63.00	69.00
Nd	7.38	122.03	47.78	56.00	23.00	25.00

*Fe_2O_3 as total iron.

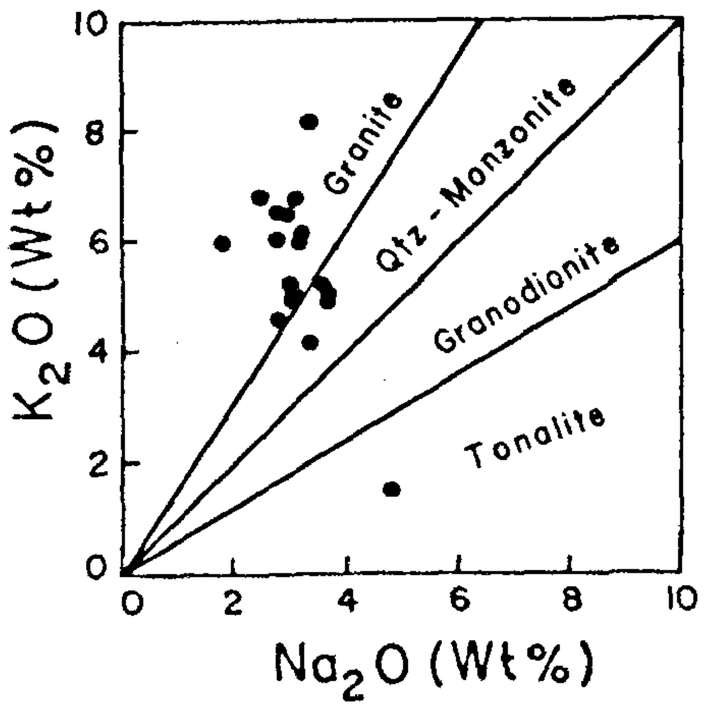

Figure 2. Na_2O–K_2O relationship in the Tirodi gneiss depicting a granitic- to quartz-monzonite character except one sample which shows tonalite character.

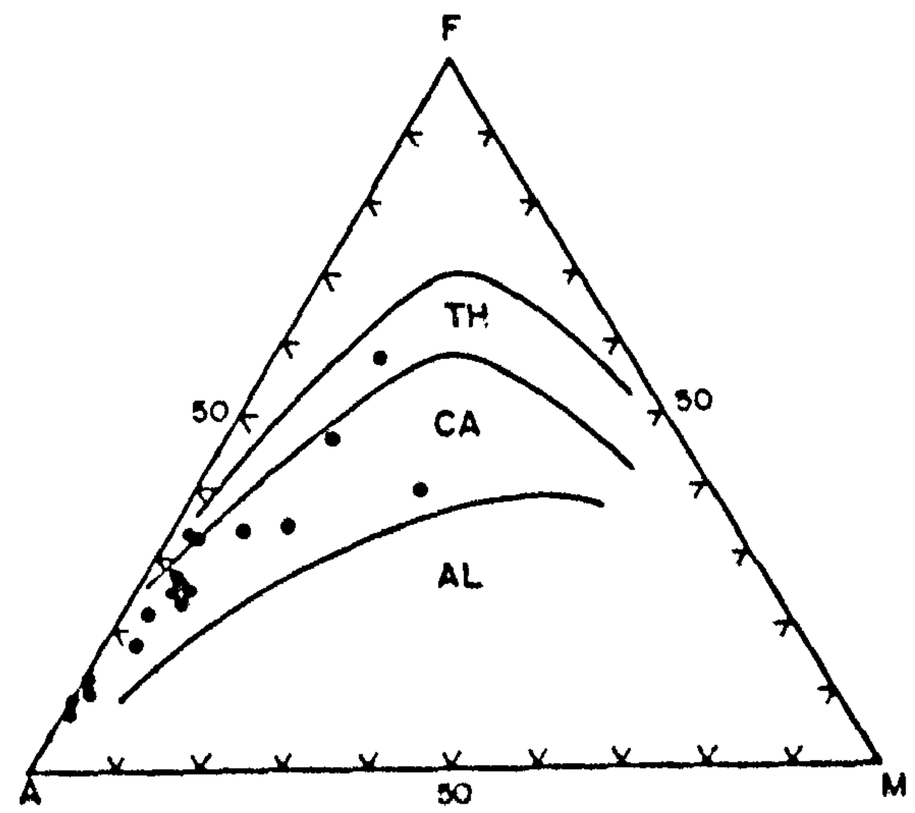

Figure 3. Alkalies – total iron as Fe_2O_3–MgO (AFM) ternary diagram showing mainly calk-alkaline fractionation trend for the protoliths of the Tirodi gneiss.

one sample with significant positive anomaly (Eu/Eu* = 0.04–1.78; Av. 0.43). ΣREE varies from 49.89 to 897.07 ppm with an average of 305.89 ppm.

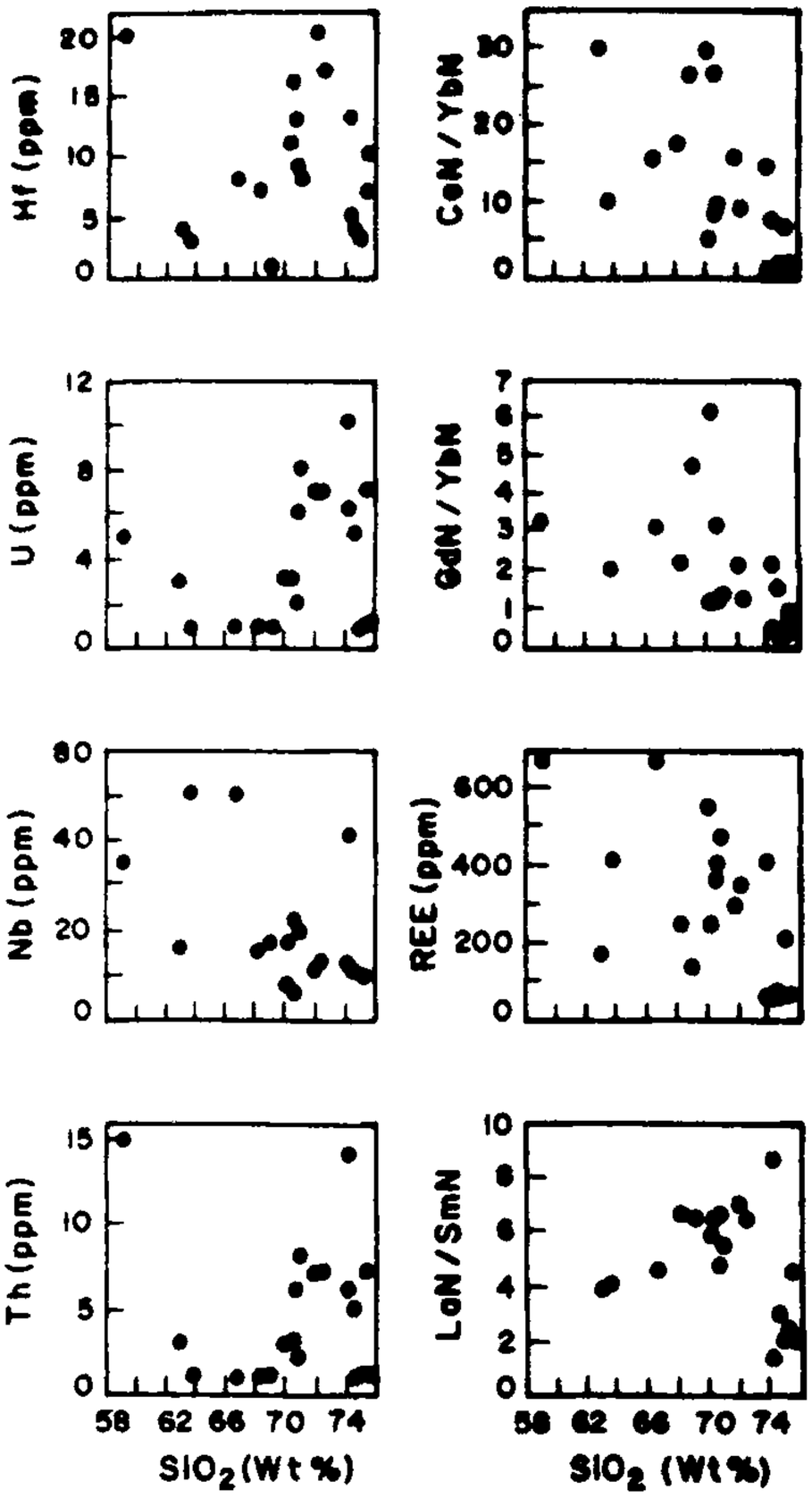

Figure 4. Variation diagram showing the relationship of SiO_2 with Th, Nb, U and Hf and REE ratios.

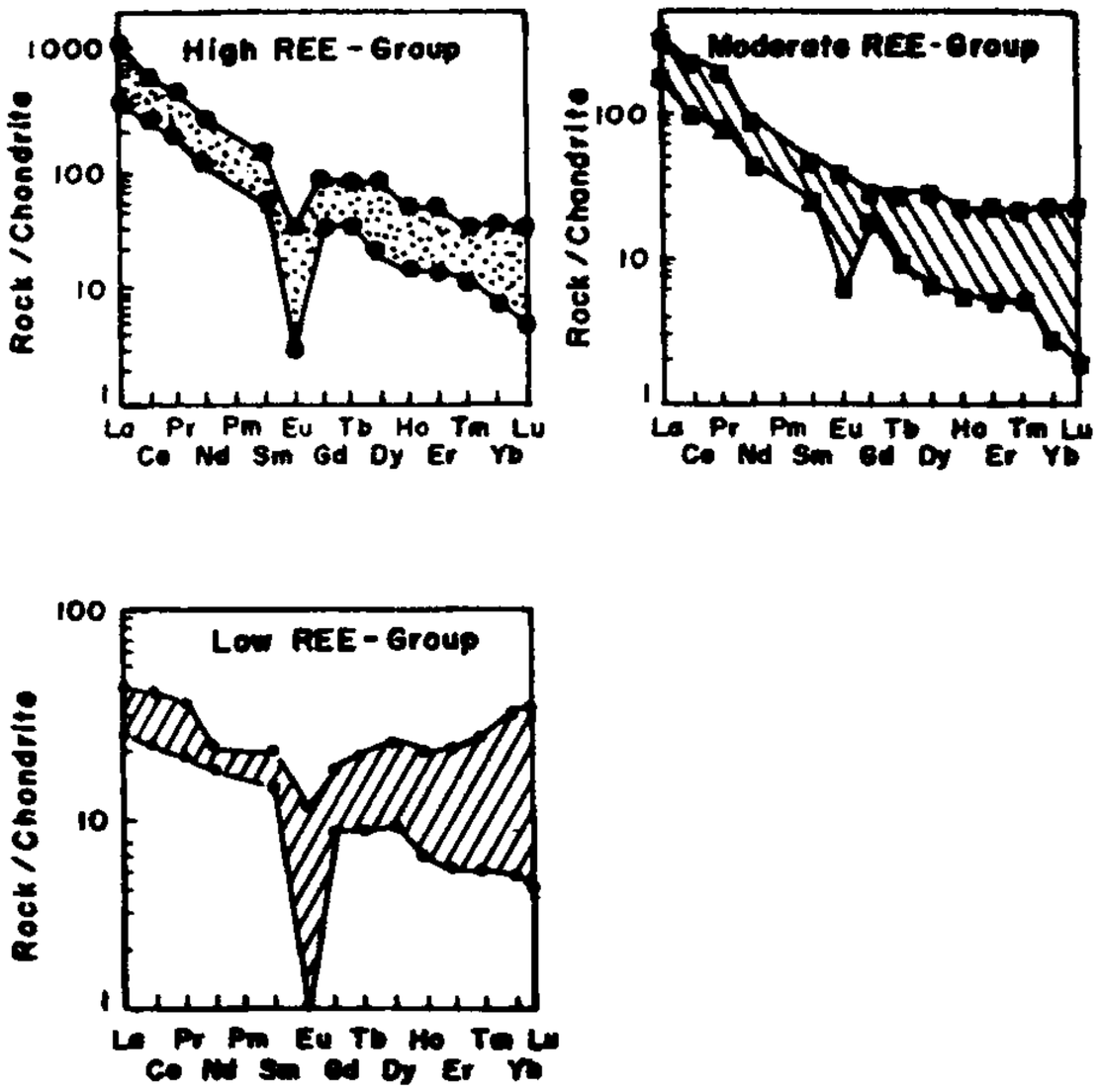

Figure 5. Chondrite normalized REE patterns of the Tirodi gneiss with all the three groups showing negative Eu anomalies of varying degrees.

K/Rb in these gneisses varies from 82 to 441, with an average K/Rb of 224, which is quite similar to the reported upper crustal K/Rb of 230. These gneisses are characterized by relatively enriched large ion lithophile elements (LILE) like K, Rb, Ba, Cs, U and Th, similar to the acid igneous rocks of the upper crustal regions.

These variations suggest that the LILE geochemistry is probably not significantly affected by post-formational changes and reflect their original nature, since these gneisses are not characterized by metamorphism of any significantly high grade. Moreover, the variations in the high field strength (HFS) elements as also the REE compositions suggest derivation from mixed and evolved source regions.

These gneisses can be divided into three groups with respect to their total REE contents and chondrite-normalized rare earth element patterns, i.e. a high REE group, a moderate REE group and a low REE group (Figure 5). Almost all the groups exhibit negative Eu anomalies (with the exception of one sample), though of different extent in the three groups, and varying degrees of LREE and HREE fractionation.

Based on the relationship of 10000*Ga/Al vs Nb, Ce, Zr and Y, most of the samples fall in the A-type granite field, with only a few samples tending to be I- and S-type granites (Figure 6). Similarly the plot of Zr + Nb + Ce + Y vs 10000*Ga/Al suggest an A-type character for these gneisses (Figure 7). On the tectonic discrimination plots, these gneisses indicate a within-plate granite (WPG) character[5], with only a few samples straddling the volcanic arc granites (VAG) and syn-collision granite (syn-COLG) fields (Figure 8). On the ternary plot involving Y-Nb-3Ga, these gneisses overwhelmingly fall in the A2 group of the A-type granites (figure not shown). They are characterized by high SiO_2, Na_2O, K_2O and are relatively low in MgO, CaO and P_2O_5. Similarly, among trace elements Rb, Zr, Y, Nb, LREE and Ga are enriched in these gneisses, while Sr, Eu, Sc, V, Ni and Cr are relatively low (Tables 1 and 2). Negative Eu anomalies, high ratios of Rb/Sr, K/Rb, Ga/Al, Zr/Ni, Y/Sc and high Zr + Nb + Y + Ce are recorded, which distinguish these gneisses from I- and S-type magmas[6–13]. All the samples have consistently high Ga values (ranging from 11 to 89 ppm) and usually high ratios of 10000*Ga/Al (1.48–10.46). The average composition of the Tirodi gneisses resembles the average 'A-type granite' in several respects (Table 3), apart from most of the samples falling in the A-type granite field

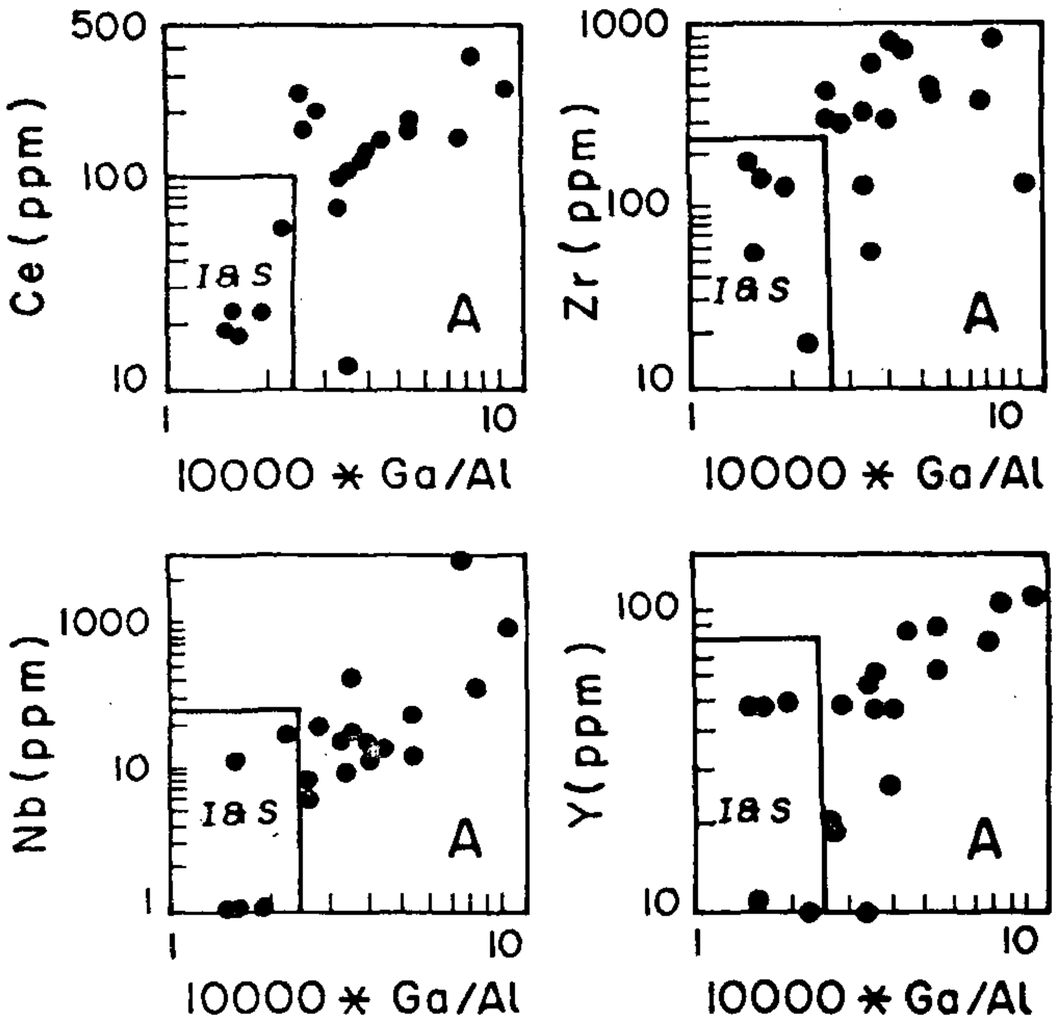

Figure 6. 10000*Ga/Al vs Nb, Ce, Y and Zr in the Tirodi gneiss suggesting their mainly A-type granite character. I, I-type granite; S, S-type granite.

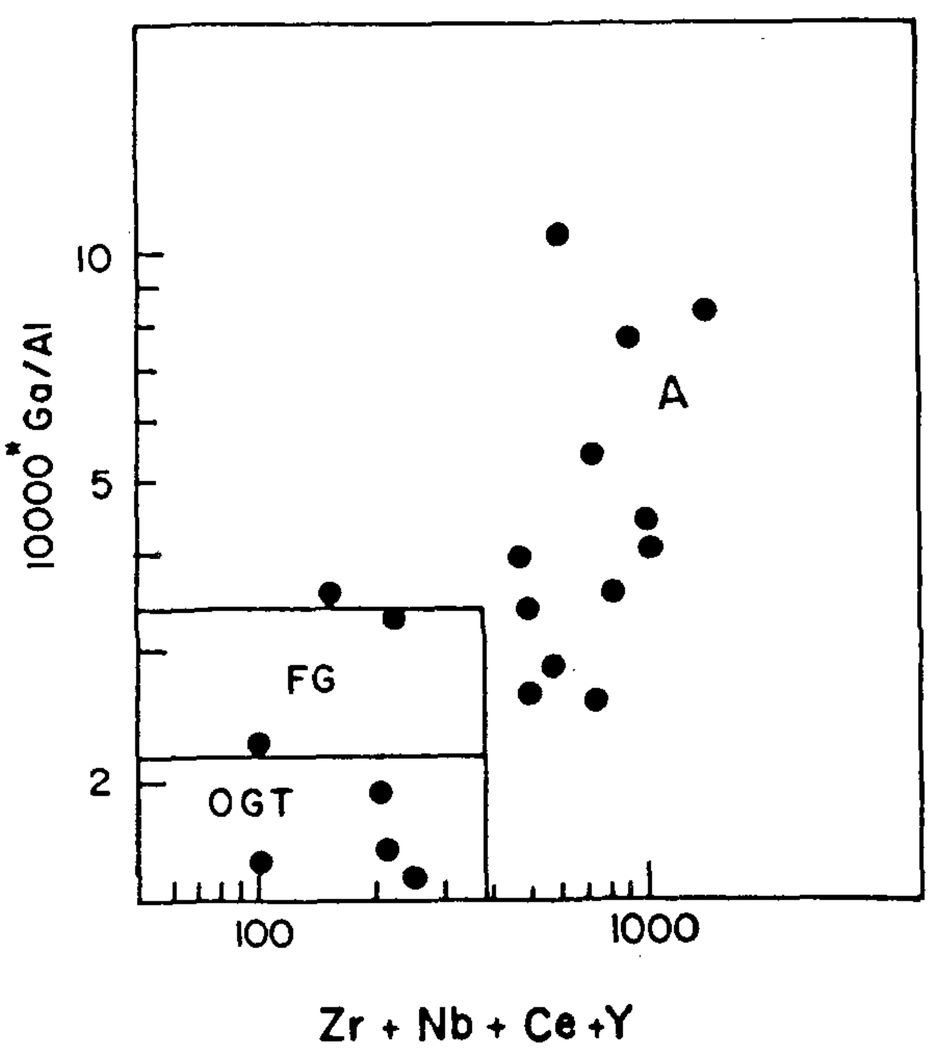

Figure 7. Zr + Nb + Ce + Y vs 10000*Ga/Al in the Tirodi gneisses indicating the predominantly A-type character of these gneisses. FG, Fractionated Granites; OGT, Other granite types.

and the 'within plate granite' side in the tectonic discrimination diagrams[5]. Enrichment in high field strength elements (HFSE) is a characteristic feature of these gneisses. The concentrations and ratios of several HFS elements which are considered relatively immobile during most alteration and metamorphic processes may be more reliable[14].

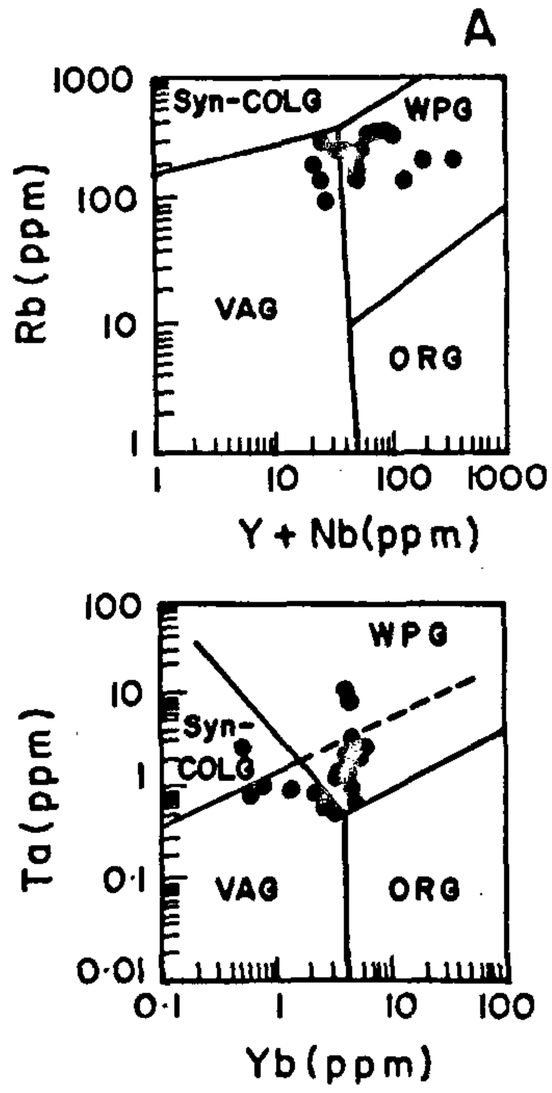

Figure 8. Tectonic discrimination diagrams (A = Y + Nb vs Rb; B = Yb vs Ta) for the Tirodi gneisses, indicating their predominantly within plate granite nature. VAG, Volcanic arc granite; syn-COLG, Syn-collision granites.

As A-type granites occur in non-orogenic settings, both within plate and along margins during the waning stages of subduction related magmatism, the possibility of a petrogenetic link between these granitic gneisses and the accretionary tectonics of the Central Indian region cannot be ruled out. The Dongargarh Super Group metavolcanics, particularly the Khairagarh volcanics are stratigraphically equivalent to the Sausars. They are considered to be the products of subduction related volcanism[15,16]. The emplacement of the volcanics might have supplied the necessary heat required for melting the lower crustal rocks. The occurrence of granulites in close proximity to these gneisses also supports the origin of the protoliths for the Tirodi gneisses from lower crustal source region. The protoliths of the Tirodi gneisses could be products of lower crustal melting. The necessary fluids required for enabling the resultant melt get enriched in the incompatible and HFS elements might have been provided by the basic magma. The Nb-Y-3Ga relationship as also the Nb-Y-Ce relationship in these gneisses suggest that they possibly belong to the A2-type granites which can form by the involvement of magma generated by continental margin and island-arc basalts, possibly during the waning stages of subduction or non-orogenic setting in a marginal basin environment. Such felsic magmas are normally produced during the rapid development of island arc/back-arc basin system via extension within the margin of a pre-existing older

continental crust. Sedimentation and magmatic activity within the basin ceases on closure of the back-arc basin and accretion of the crust in the Proterozoic[14].

A-type granite plutonism usually, though not exclusively, occurs in rift related environments in continental crustal regions. The production of anorogenic granite magma requires: (i) a source of dehydrated, reasonably salic crust; (ii) a source of heat sufficient to partially melt this crust; and (iii) a conduit to lead the magma to a higher level[9,10]. Such a scenario could be envisaged for the petrogenesis of the protoliths of the Tirodi gneisses. A plausible petrogenetic model for the origin of the protoliths for these granitic gneisses could be their derivation by extended fractional crystallization of a melt generated at lower crustal levels, contemporaneous with basalt emplacement in a rift-related extensional environment. Initial deposition of the sedimentary sequence of the Sausar Group might have started prior to the emplacement of the granitic melt, leading to a limited assimilation of the sediments already in place. That is possibly why some samples of the Tirodi gneiss unit tend towards the 'syn-collision' and 'volcanic arc' granite fields on the tectonic discrimination diagrams (Figure 8) and show a limited affinity towards the I- and S-type granites (Figure 6), though the overall A-type character is evident. There is a general high degree of concordance between Y/Nb and Yb/Ta ratios, which is the case in several A-type granite suites. Similarly Y-Yb and Nb-Ta show geochemically similar behaviour and these pairs of elements show concordance, as is also the case in several A-type granites. A detailed look at the overall and average compositions of the Tirodi gneiss unit brings out the remarkable similarities in several respects to the A-type granite (Table 3). The similarities are more striking in the case of CaO, Iron, Na_2O, K_2O, Ga, Rb, Y, Zr, La, Ce and Nd. Enrichment of HFS elements is a characteristic feature of these gneisses like in the A-type granites. The geochemical fingerprints in the Tirodi gneisses as mentioned above are consistent with the mixing of a newly mantle-derived component with an older crustal component through lower crustal assimilation and possibly the sediments of the Sausar Group on a limited scale, as suggested by the somewhat lower levels of Ba, U and Th and the moderate-to-high Al_2O_3 levels in these gneisses compared to the average A-type granite and the fact that some samples of these gneisses fall outside the 'A-type granite' and 'within plate granite' fields (Figure 6). The lithological configuration of the Central Indian craton suggests such a tectonic environment as can be seen from the occurrence of the subduction-related basic volcanism and the amphibolites which exhibit formation in a continental margin tectonic setting and a back-arc basin tectonic environment respectively[16,17].

1. Mohanty, S., *J. Geol. Soc. India*, 1998, **60**, 200–210.
2. Mohanty, S., *J. Geol. Soc. India*, 1993, **41**, 55–61.
3. Phadke, A. V., in *Precambrian of Central India*, G.S.I. Special Publication, 1990, **28**, pp. 287–302.
4. Sarkar, S. N., Trivedi, J. R. and Gopalan, K., *J. Geol. Soc. India*, 1986, **27**, 30–31.
5. Pearce, J. A., Harris, N. B. W. and Tindle, A. G., *J. Petrol.*, 1984, **25**, 956–983.
6. Loiselle, M. C. and Wones, D. R., *Geol. Soc. Am. Bull. Abstr. Prog.*, 1979, **92**, 468.
7. Collins, W. J., Beans, S. D., White, A. J. R. and Chappell, B. W., *Contrib. Mineral. Petrol.*, 1982, **80**, 189–200.
8. Clemens, J. D. and Wall, V. J., *Am. Mineral.*, 1984, **71**, 317–324.
9. Whalen, J. B., Currie, K. and Chappell, B. W., *Contrib. Mineral. Petrol.*, 1987, **95**, 407–419.
10. Eby, G. N., *Lithos*, 1990, **26**, 115–134.
11. Creaser, R. A., Price, R. C. and Wormald, R. J., *Geology*, 1991, **19**, 163–166.
12. Turner, S. P., Foden, F. D. and Morrison, R. S., *Lithos*, 1992, **28**, 151–179.
13. Whalen, J. B., Jenner, G. A., Longstaffe, J., Robert, F. and Gariepy, C., *J. Petrol.*, 1996, **37**, 1463–1489.
14. Ashley, P. M., Cook, N. D. J. and Fanning, C. M., *Lithos*, 1996, **38**, 167–184.
15. Yedekar, D. B., Jain, S. C., Nair, K. K. K. and Dutta, N. K., in *Precambrian of Central India*, G.S.I. Special Publication, 1990, **28**, 1–43.
16. Subba Rao, M. V., Narayana, B. L., Mallikharjuna Rao, J., Rama Rao, P., Divakara Rao, V., Reddy, G. L. N. and Murthy, N. N., *DCS Newsl.*, 1995, **5**, 11–13.
17. Subba Rao, M. V., Narayana, B. L. and Divakara Rao, V., *Annu. Conv. Indian Geophys. Union* (abs) 1995, **32**, 138–139.

ACKNOWLEDGEMENTS. We are grateful to the Director, NGRI for encouragement and kind permission to publish the paper. This work was carried out under a project funded by DST. The help of Drs P. K. Govil and V. Balaram in major and trace element analyses respectively is thankfully acknowledged.

Received 18 May 1998; revised accepted 18 February 1998